Investigation of free vibration characteristics for skew multiphase magneto-electro-elastic plate

M. C. Kiran, and S. Kattimani

Citation: AIP Conference Proceedings **1943**, 020015 (2018); doi: 10.1063/1.5029591
View online: https://doi.org/10.1063/1.5029591
View Table of Contents: http://aip.scitation.org/toc/apc/1943/1
Published by the American Institute of Physics

Investigation of Free Vibration Characteristics for Skew Multiphase Magneto-Electro-Elastic Plate

M. C. Kiran [1, a)] and S Kattimani[1, b)]

[1]*Department of Mechanical Engineering, National Institute of Technology, Karnataka, Surathkal - 575025, India.*

[a)] 20.kiranmc@gmail.com
[b)]Corresponding author: sck@nitk.ac.in

Abstract. This article presents the investigation of skew multiphase magneto-electro-elastic (MMEE) plate to assess its free vibration characteristics. A finite element (FE) model is formulated considering the different couplings involved via coupled constitutive equations. The transformation matrices are derived to transform local degrees of freedom into the global degrees of freedom for the nodes lying on the skew edges. Effect of different volume fraction (V_f) on the free vibration behavior is explicitly studied. In addition, influence of width to thickness ratio, the aspect ratio, and the stacking arrangement on natural frequencies of skew multiphase MEE plate investigated. Particular attention has been paid to investigate the effect of skew angle on the non-dimensional Eigen frequencies of multiphase MEE plate with simply supported edges.

INTRODUCTION

The growing demand for smarter composite structures in aerospace, marine application, sensors, and actuators has accelerated the research in the domain of smart composite materials recently. Such composites possess several unique characteristics. Their structural response to the applied load has become an important research topic. Magneto-electro-elastic (MEE) composites composed of piezoelectric ($BaTiO_3$) and magnetostrictve ($CoFe_2O_4$) materials are one amongst many smart structural composites. The MEE composites facilitate conversion of energy between electric and magnetic fields via magneto-electric effect which is absent in their individual constituents (i.e. Pure piezoelectric and magnetostrictive phases). Though many researchers have contributed to the studies on MEE composites, Suchtelen [1] was first to report the magneto-electric effect in MEE composites. Later, the study of structural behavior with more highlight on plates, shells, and beams were well reported [2 – 4]. Exact solutions for fiber reinforced MEE a thin plate with closed circuit electric restriction was presented by Liu [5]. Free vibrations of three dimensional multilayered MEE for clamped boundary condition was thoroughly investigated by Chen et al [6]. Kattimani and Ray [7 – 9] investigated on the geometrically nonlinear vibration control of MEE plates and shells using 1-3 piezoelectric composite. Ding and Jiang [10] investigated the simply supported annular MEE plate using the boundary element method. Ramirez et al. [11, 12] adopted a discrete layer model to study the free vibration behaviour of MEE laminates and graded plates. Feng and Su [13] investigated the dynamics of FG MEE plate containing an internal crack. Simões [14] reported the static and free vibration of MEE plates using a higher - order model. Phoenix [15] studied the multi-layered plates for static and dynamic conditions using layer-wise mixed FE method. Biju et al. [16] investigated the effect of magnetic vector on the dynamic behaviour of moderately thick MEE plate. Alaimo et al. [17] presented an equivalent single layer model to study the multilayerd MEE plate. A Reissner–Mindlin model for FG multilayered MEE laminates has been developed by Zhong et al. [18]. Alaimo [19] discussed a novel FE formulation to sudy the large deflections in MEE multilayered plates. The semi-analytical solutions were developed by Xin and Hu [20] for the free vibration studies of multilayered MEE plates. Vinyas and Kattimani [21 – 23] studied the static behaviour of stepped functionally graded MEE plates and beams.

Skew plates and laminates find a prominent presence in many engineering applications. Skew composite plate exhibit far superior structural behavior over it peers for the identical mass of the normal plate. All these unique properties have been successful in attracting the attention of many researchers. Studies on free vibration of skew plates have been extensively carried out. Garg et al. [24] investigated vibration analysis of different skew laminates using a higher-order shear deformation theory. Kanasogi and Ray [25] have studied the active vibration control for different layups of skew composite plate. Free vibration characteristics of

Advances in Mechanical Design, Materials and Manufacture
AIP Conf. Proc. 1943, 020015-1–020015-7; https://doi.org/10.1063/1.5029591
Published by AIP Publishing. 978-0-7354-1638-3/$30.00

isotropic skew plates were investigated using the Rayleigh-Ritz method [26 – 29]. The extensive literature review provides a larger insight over free vibration of MEE composite plates and laminated composite plates with skewed edges. However, skew multiphase MEE plate has not been investigated and provides an ample scope for further research. It is noteworthy to mention that to the best of the author's knowledge, the research concerning the multiphase MEE plate with skewed edges has not been reported in the open literature. Hence, this paper presents the FE formulation to investigate the free vibration characteristics o skew multiphase MEE plate. The effect of aspect ratio, width to thickness ratio and stacking sequence on the free vibration behavior has been investigated thoroughly.

PROBLEM DESCRIPTION AND GOVERNING EQUATION

A schematic representation of multiphase magneto-electro-elastic (MMEE) plate with skewed edges having length a, width b, total thickness H and skew angle α is depicted in Fig. 1. The different volume fraction (V_f) of $BaTiO_3$ is depicted in the figure. The cartesian coordinate system is represented by (x, y, z) and (x', y', z') are the local coordinates at skew angle α of the skew MMEE plate.

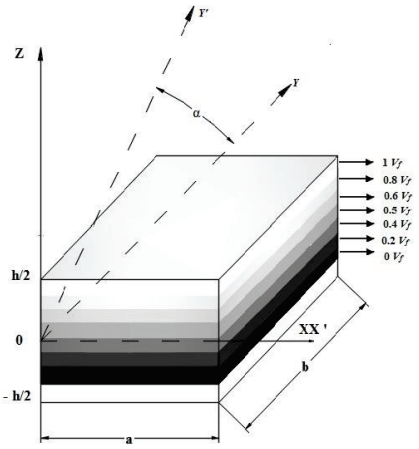

FIGURE 1. Schematic representation of the skew MMEE plate

Finite element selection

Finite element modelling is based on the idea of considering a structure as an assembly of element linked through nodes. In the present work an eight node iso-parametric quadrilateral serendipity element is considered. The shape functions for the element are given by

$$\begin{aligned} n_1 &= -\frac{1}{4}(1-\xi)(1-\eta)(1+\xi+\eta) & n_4 &= -\frac{1}{2}(1-\xi)(1-\eta^2) & n_7 &= -\frac{1}{2}(1-\xi^2)(1-\eta) \\ n_2 &= -\frac{1}{2}(1-\xi^2)(1-\eta) & n_5 &= -\frac{1}{2}(1+\xi)(1-\eta^2) & n_8 &= -\frac{1}{4}(1+\xi)(1+\eta)(1-\xi-\eta) \\ n_3 &= -\frac{1}{4}(1+\xi)(1-\eta)(1-\xi+\eta) & n_6 &= -\frac{1}{4}(1-\xi)(1+\eta)(1+\xi-\eta) \end{aligned} \quad (1)$$

Displacement field

The displacement fields can be expressed as

$$\begin{aligned} u_i(x, y, z) &= u_{0i}(x, y) + z\ \theta_i(x, y) \\ w(x, y, z) &= w_0(x, y) + z\ \theta_z(x, y) + z^2\ \zeta_z(x, y) \end{aligned} \quad (2)$$

where i = x and y, $u_x = u$, $u_y = v$, $u_{0x} = u_0$, $u_{0y} = v_0$. In the above displacement fields, u0, v0 and w0 are the mid-plane displacements of the MEE plate with skewed edges while, θ_x and θ_y are shear displacements. θ_z and ζ_z refer to the rotational displacements about z- direction of the plate. As thin structures being more susceptible to shear locking, the strain component are considered separately for bending and shearing to study the effect of transverse

shear deformation individually. The strain vectors associated with the displacement field in Eq. (2) at any point in the plate can be expressed as follows:

$$\{\varepsilon_b^k\} = \{\varepsilon_{bt}\} + [R_1]\{\varepsilon_{rb}\}\ ,\ \{\varepsilon_s^k\} = \{\varepsilon_{ts}\} + [R_2]\{\varepsilon_{rs}\} \tag{3}$$

wherein k represents the layer number for the plate, [R1] and [R2] defines the transformation matrices; while the strain vectors appearing in Eq. (3) are given as follows:

$$\{\varepsilon_{bt}\} = \left[\frac{\partial u_0}{\partial x} \quad \frac{\partial v_0}{\partial y} \quad 0 \quad \frac{\partial u_0}{\partial y} + \frac{\partial v_0}{\partial x}\right],\ \{\varepsilon_{ts}\} = \left[\frac{\partial w_0}{\partial x} \quad \frac{\partial w_0}{\partial y}\right] \text{ and}$$

$$\{\varepsilon_{rb}\} = \left[\frac{\partial \theta_x}{\partial x} \quad \frac{\partial \theta_y}{\partial y} \quad \frac{\partial \theta_x}{\partial x} + \frac{\partial v_0}{\partial x} \quad \theta_z \quad \zeta_z\right]$$

Constitutive equation

The constitutive equations considering the effect of coupled fields, for the MMEE plate with skewed edges can be written as

$$\{\sigma_b^k\} = [\bar{Q}_b^k]\{\varepsilon_b^k\} - \{e_b^k\}E_z - \{q_b^k\}H_z\ ,\ \{\sigma_s^k\} = [\bar{Q}_s^k]\{\varepsilon_s^k\} \tag{4a}$$

$$D_z = \{e_b^k\}^T\{\varepsilon_b^k\} + \in_{33}^k E_z + d_{33} H_z \tag{4b}$$

$$B_z = \{q_b^k\}^T\{\varepsilon_b^k\} + d_{33}^k E_z + \mu_{33} H_z \tag{4c}$$

where k = 1, 2, 3 designates the layer number from the bottom layer to the top and

$$[\bar{Q}_b^k] = \begin{bmatrix} \bar{Q}_{11}^k & \bar{Q}_{12}^k & \bar{Q}_{13}^k & \bar{Q}_{16}^k \\ \bar{Q}_{12}^k & \bar{Q}_{22}^k & \bar{Q}_{23}^k & \bar{Q}_{26}^k \\ \bar{Q}_{13}^k & \bar{Q}_{23}^k & \bar{Q}_{33}^k & \bar{Q}_{36}^k \\ \bar{Q}_{16}^k & \bar{Q}_{26}^k & \bar{Q}_{36}^k & \bar{Q}_{66}^k \end{bmatrix},\ [\bar{Q}_s^k] = \begin{bmatrix} \bar{Q}_{55}^k & \bar{Q}_{45}^k \\ \bar{Q}_{45}^k & \bar{Q}_{44}^k \end{bmatrix} \tag{5}$$

where, $[\bar{Q}_b^k]$ and $[\bar{Q}_s^k]$ being the transformed coefficient matrices, $\in_{33}^k$, μ_{33} and d_{33} are the dielectric, the magnetic permeability and the electromagnetic coefficient, respectively. D_z, E_z, B_z, and H_z represents the electric displacement, the electric field, the magnetic induction, and the magnetic field, respectively. $\{e_b^k\}$ and $\{q_b^k\}$ represents the electric coefficient matrix and the magnetic coefficient matrix, respectively.

Governing equation

Using the principle of virtual work, the governing equations for the MMEE plate with skewed edges can be established as

$$\sum_{k=1}^{3}\left(\int_{\Omega^k}\delta\{\varepsilon_b^k\}\{\sigma_b^k\}d\Omega^k + \int_{\Omega^k}\delta\{\varepsilon_s^k\}\{\sigma_s^k\}d\Omega^k + \int_{\Omega^k}\delta\{d_t\}^T\rho^k\{\ddot{d}_t\}d\Omega^k\right) - \int_{\Omega^k}\delta E_z^k D_z^k d\Omega^k - \int_{\Omega^k}\delta H_z^k B_z^k d\Omega^k = 0 \tag{6}$$

where, Ω^k (k = 1, 2, 3) indicates the volume of the respective layer, ρk denotes the mass density of the kth layer. The transverse electric field and the electric potential, the transverse magnetic field and the magnetic potential related correspondingly in accordance with the Maxwell's equation.

Skew boundary transformation

For the skewed MMEE plates, the displacements along the skew edges lying in the local coordinate need to be transformed into the global coordinate to facilitate the proper imposition of boundary conditions. The transformation is achieved by the simple relations given as follows:

$$\{d_t\} = [L_t]\{d_t^l\}\ ,\ \{d_r\} = [L_r]\{d_r^l\} \tag{7}$$

$$\{d_t^l\} = [u_0^l\ v_0^l\ w_0^l]^T\ ,\ \{d_r^l\} = [\theta_x^l\ \theta_y^l\ \theta_z^l\ \zeta_z^l]^T \tag{8}$$

Where, d_t , d_r and d_t^l , d_r^l are the generalised displacements on the global and the local edge coordinate system, respectively. $[S_t]$ and $[S_r]$ are the transformation matrices for a node on the skew boundary and are given by

$$[S_t]=\begin{bmatrix} m & n & 0 \\ -n & m & 0 \\ 0 & 0 & 1 \end{bmatrix},\ [S_r]=\begin{bmatrix} m & n & 0 & 0 \\ -n & m & 0 & 0 \\ 0 & 0 & 1 & 0 \\ 0 & 0 & 0 & 1 \end{bmatrix} \tag{9}$$

where, m = cosα and n = sinα. It may be noted that the transformation is not required for the nodes not lying on the skew edges and the diagonal elements of the transformation matrices are considered to be unity for such cases.

Free vibration behavior

Using eqations (6) - (8) the final global equations of motion are obtained as follows:

$$[M]\{\ddot{d}_t\}+\left([K_1]-[K_2][K_3]^{-1}[K_2]^T\right)\{d_t\}=\{F_t\}$$

$$[M]\{\ddot{d}_t\}+[K]\{d_t\}=\{F_t\}$$

$$\text{and } [K]=\left([K_1]-[K_2][K_3]^{-1}[K_2]^T\right) \tag{10}$$

where, the global aggrandized matrices are given as follows:

$$[K_1]=[k_{tt}^g]+[k_{t\phi}^g][k_{\phi\phi}^g]^{-1}[k_{t\phi}^g]^T+[k_{t\psi}^g][k_{\psi\psi}^g]^{-1}[k_{t\psi}^g]^T,$$

$$[K_2]=[k_{tr}^g]+[k_{t\phi}^g][k_{\phi\phi}^g]^{-1}[k_{r\phi}^g]^T+[k_{t\psi}^g][k_{\psi\psi}^g]^{-1}[k_{r\psi}^g]^T,$$

$$[K_3]=[k_{rr}^g]+[k_{r\phi}^g][k_{\phi\phi}^g]^{-1}[k_{r\phi}^g]^T+[k_{r\psi}^g][k_{\psi\psi}^g]^{-1}[k_{r\psi}^g]^T.$$

The eigenvalue problem can be formulated considering the global equations of motion in terms of global translational degrees of freedom as follows:

$$[K]+\lambda[M]=0 \tag{11}$$

where, [K] is the global stiffness matrix, [M] is the global mass matrix and λ is the eigenvalue ie., $\lambda = \omega 2$.

RESULTS AND DISCUSSIONS

The response of MMEE plate with skewed edges under simply supported boundary conditions is studied to analyse the free vibration behavior. The effect of volume fraction, stacking sequence and other geometrical parameters for different skew angles are presented. The properties corresponding to different volume fraction are taken from the studies of Vinyas and Kattimani [21].The layer thickness is taken as 0.05 m, whereas the length and the width are considered to be 1 m. The non-dimensional natural frequencies are obtained using the relation

$$\bar{\omega}=\omega a\sqrt{\rho_{max}/C_{max}} \tag{12}$$

where, ρ_{max} corresponds to maximum density and C_{max} corresponds to the maximum elastic constant.

Validation

The proposed FE model in the preceding section is verified with a semi-analytical model for the multilayered MEE plate [6]. The natural frequencies of MEE plate for identical testing parameters are extracted from the present FE model and compared with the reference results in Table 1. To the author's best knowledge free vibration analysis of MEE skew plates are not available in open literature. Hence to verify the effectiveness of the developed model for the skew plates, non-dimensional natural frequencies of the skew laminated composites obtained by Garg et al. [24] is considered and compared in Table 2. It may be observed from Table 1 and 2 that, the results obtained using the present finite element formulation are in very good agreement with results reported by Chen et al.[6] and Garg et al.[24].

TABLE 1. Non-dimensional frequency parameter $\lambda = \omega b^2 / \pi^2 h (\rho/E_2)^{1/2}$ for the clamped-clamped laminated composite plate (a/h=10).

Skew angle (α)	Source	Antisymmetric cross-ply ($0^0/90^0/0^0/90^0$)			Symmetric cross-ply ($90^0/0^0/90^0/0^0/90^0$)		
		Modes			Modes		
		1	2	3	1	2	3
	Ref. [24]	2.2990	3.7880	3.7880	2.3687	3.5399	4.1122
0^0	Present	2.2590	3.5213	4.2695	2.2400	3.3655	4.2382
	Ref. [24]	2.3809	3.7516	4.0785	2.4663	3.6255	4.3418
15^0	Present	2.2992	3.4560	4.2841	2.2860	3.3637	4.2346
	Ref. [24]	2.6666	3.9851	4.7227	2.7921	3.9557	5.0220
30^0	Present	2.4403	3.5067	4.3609	2.4396	3.4363	4.2949
	Ref. [24]	3.3015	4.6290	5.8423	3.4739	4.7129	5.8789
45^0	Present	2.7348	3.7102	4.6270	2.7439	3.6545	4.6862

TABLE 2. Non-dimensional normalized natural frequency modes for clamped-clamped B/F/B plate

Source	Normalized natural frequency						
	1	2	3	4	5	6	7
Present	1.3107	2.1727	2.1727	2.6383	2.6383	2.7142	2.9750
Ref. [6]	1.3452	2.2231	2.2231	2.6178	2.6178	2.9404	2.9939

Eigen frequencies evaluation of skew MMEE plates

This section presents the free vibration characteristics of skew MMEE plate. The simply-supported MMEE plate (both single layer and multi layer) considered for the analysis has the following geometry: a = b = 1, h =0.05, and α varies from 0^0 to 45^0. The volume fraction of $BaTiO_3$ is varied from 0 to 1 i.e., $V_f = 0$ corresponds to pure $CoFe_2O_4$ phase and $V_f = 1$ corresponds to pure $BaTiO_3$ phase. The normalized natural frequencies for different volume fractions of $BaTiO_3$ over different skew angle are presented in Table 3. It can be seen from the table that the natural frequency increases with the decrease in the volume of $BaTiO_3$. It can also be seen that the natural frequencies increase with the increase in skew angle and a sharp increase in frequency witnesses for $\alpha = 45^0$. Further, a layered multiphase MMEE plate is analysed. The seven layers of MMEE plate with the volume fraction stacking sequence of 0, 0.2, 0.4, 0.5, 0.6, 0.8, and 1 is considered for the analysis. Table 4 presents the natural frequencies for the seven layered skew MMEE plate for different skew angle. The natural frequencies of the layered MMEE plate are larger than the single layer multiphase plate. It can be inferred that the layered plate attains higher stiffness in comparison with a single layer MMEE plate. In addition, the natural frequencies increase with the increase in skew angle and a sharp increase in frequency witnesses for $\alpha = 45^0$. The influence of aspect ratio and thickness ratio on MMEE plate with $\alpha = 45^0$ is presented in Table 5 and Table 6, respectively. It can be seen that the increase in aspect ratio and the thickness ratio decreases the natural frequency. However, a meagre difference in the natural frequency is observed for higher aspect ratio and thickness ratio, respectively while, the difference is larger for lower aspect and thickness ratio.

TABLE 3. Influence of volume fraction and skew angle on single layer skew MMEE plate

Skew angle	V_f	Modes				
		1	2	3	4	5
	1	0.2230	0.5541	0.5541	0.8890	1.1259
	0.8	0.2275	0.5661	0.5661	0.9106	1.1524
	0.6	0.2336	0.5818	0.5818	0.9373	1.1853
0^0	0.5	0.2356	0.5866	0.5866	0.9453	1.1952
	0.4	0.2334	0.5821	0.5821	0.9410	1.1891
	0.2	0.2307	0.5772	0.5772	0.9406	1.1856
	0	0.2487	0.6205	0.6205	1.0037	1.2668
	1	0.2506	0.5566	0.6459	0.9200	1.2029
	0.8	0.2565	0.5693	0.6609	0.9433	1.2325
	0.6	0.2640	0.5855	0.6799	0.9715	1.2685
	0.5	0.2662	0.5905	0.6857	0.9798	1.2792
15^0	0.4	0.2650	0.5869	0.6817	0.9769	1.2743
	0.2	0.2648	0.5840	0.6788	0.9795	1.2743
	0	0.2827	0.6261	0.7272	1.0420	1.3581
	1	0.3367	0.6462	0.8764	1.0533	1.4681
	0.8	0.3455	0.6625	0.8991	1.0833	1.5079
	0.6	0.3559	0.6823	0.9260	1.1176	1.5541
	0.5	0.3589	0.6882	0.9340	1.1274	1.5675
30^0	0.4	0.3588	0.6861	0.9322	1.1290	1.5663
	0.2	0.3614	0.6870	0.9353	1.1429	1.5769
	0	0.3823	0.7322	0.9940	1.2046	1.6703
	1	0.5261	0.8777	1.3784	1.3852	1.8633
	0.8	0.5398	0.9016	1.4216	1.4243	1.9172
	0.6	0.5555	0.9292	1.4680	1.4684	1.9821
	0.5	0.5600	0.9372	1.4804	1.4813	2.0045
45^0	0.4	0.5606	0.9373	1.4831	1.4896	1.9946
	0.2	0.5656	0.9446	1.4994	1.5213	1.9500
	0	0.5953	0.9990	1.5782	1.5879	2.1746

TABLE 4. Influence of skew angle on seven layer skew MMEE plate

Skew angle	**Modes**				
	1	**2**	**3**	**4**	**5**
0^0	0.2693	0.6683	0.6708	1.0782	1.3631
15^0	0.3046	0.6741	0.7828	1.1179	1.4604
30^0	0.4111	0.7865	1.0674	1.2885	1.7925
45^0	0.6428	1.0738	1.6955	1.6974	2.2431

TABLE 5. Influence of aspect ratio (b/a) on seven layer skew MMEE plate

b/a ratio	**Modes ($\alpha = 45^0$)**				
	1	**2**	**3**	**4**	**5**
0.5	1.7722	2.1448	2.1528	2.9208	4.2589
1	0.6428	1.0738	1.6955	1.6974	2.2431
1.5	0.4145	0.7342	1.1886	1.2220	1.6044
2	0.3420	0.5475	0.9128	1.1257	1.1288
2.5	0.3125	0.4510	0.7394	0.8616	1.0591
3	0.2982	0.3973	0.6259	0.6949	0.8945

TABLE 6. Influence of thickness ratio (a/h) on seven layer skew MMEE plate

a/h ratio	Modes ($\alpha = 45^0$)				
	1	2	3	4	5
10	1.1076	1.8304	2.2430	2.5892	2.7054
20	0.6428	1.0738	1.6955	1.6974	2.2431
50	0.2934	0.4914	0.7720	0.8602	1.2187
100	0.2880	0.4878	0.7679	0.8570	1.1112

CONCLUSIONS

In this research article, the influence of volume fraction and skew angle on the free vibration characteristics of skew MMEE plate is investigated using finite element method. The substantial influence of volume fraction of $BaTiO_3$ on the natural frequency of the MMEE plate is seen. The natural frequency increases with the increase in skew angle and the rise is sharp for $\alpha = 45^0$. The geometrical parameters such as aspect ratio and thickness ratio are seen to have a significant influence on the free vibration behavior of skew MMEE plate.

REFERENCES

1. Van Suchtelen J. Philips Res. Repts, 1972, **27**, 28–37.
2. Pan E., Journal of Applied Mechanics, 2001, **68**, 608–18.
3. Pan E, Heyliger P. R., Journal of Sound and Vibration, 2002, **252**(3), 429–42.
4. Pan E. and Han F., International Journal of Engineering Science, 2005, **43**, 321-339.
5. Mei-Feng Liu, Applied Mathematical Modelling, 2011, **35**, 2443-2461.
6. Chen J. Y, Heyliger P. R and Pan E., Journal of Sound and Vibration, 2014, **333**, 4017-4029.
7. Kattimani S.C. and Ray M.C., International Journal of Mechanical Sciences, 2015, **99**, 154-167.
8. Kattimani S.C. and Ray M.C., Composite Structures, 2014b, **114**, 51-63.
9. Kattimani S.C. and Ray M. C., International Journal of Mechanics and Materials in Design, 2014a, **10**, 351-378.
10. Ding H J, Jiang A M. Science in China, Series E: Technological Sciences 2003,**46**(6), 607-19.
11. Ramirez, F H., Paul R., Pan, E. Mechanics of Advanced Materials and Structures 2006, **13**(3), 249-66.
12. Ramirez, F H., Paul R., Pan E. Journal of Sound and Vibration 2006, **292**(3), 626-44.
13. Feng W J., Su R K L. European Journal of Mechanics, A/Solids 2007, **26**(2), 363-79.
14. Simões M., José M., Mota S., Cristóvão M., Mota S., Carlos A. Composite structures 2009, **91**(4), 421-26.
15. Phoenix S S., Satsangi S K., Singh B N. Journal of Sound and Vibration 2009, **324**(3), 798-815.
16. Biju B., Ganesan N., Shankar K. International Journal of Mechanics and Materials in Design 2012, **8**(4), 349-58.
17. Alaimo A., Milazzo A., Orlando C. Computers & Structures 2013, **129**, 120-33.
18. Zhong Y F., Chen L., Yu, W B., Zhou X P., Zhang L G. Composite Structures 2013, **96**, 786-98.
19. Alaimo A., Benedetti I., Milazzo A. Composite Structures 2014, **107**, 643-53.
20. Xin L, Hu Z. Composite Structures 2015, **121**, 344-50.
21. Vinyas, M. and Kattimani, S.C., Composite Structures 2017, **178**, 63-86.
22. Vinyas, M. and Kattimani, S.C, Structural Engineering Mechanics 2017, **62**, 519-535.
23. Vinyas, M. and Kattimani, S.C., Coupled System Mechanics 2017, **6**, 351-367.
24. Ajay Kumar Garg, Rakesh Kumar Khare, Tarun Kant, Journal of Sandwich Structures and Materials, 2006, **8**, 33-53.
25. Kanasogi R. M. and Ray M. C., Journal of Composites, 2013, Hindawi Publishing Corporation.
26. Barton M. V. American Society of Mechanical Engineers Journal of Applied Mechanics, 1951, **18**, 129-134.
27. Durvasula S., Journal of Aircraft, 1969, **6**, 66-68.
28. Chopra I. and Durvasula S., International Journal of Mechanical Sciences, 1971, **13**, 935-944.
29. Nair P. S. and Durvasula S. 1973, **26**, 1-19.